

Green Chemistry

Accepted Manuscript



This is an *Accepted Manuscript*, which has been through the Royal Society of Chemistry peer review process and has been accepted for publication.

Accepted Manuscripts are published online shortly after acceptance, before technical editing, formatting and proof reading. Using this free service, authors can make their results available to the community, in citable form, before we publish the edited article. We will replace this *Accepted Manuscript* with the edited and formatted *Advance Article* as soon as it is available.

You can find more information about *Accepted Manuscripts* in the [Information for Authors](#).

Please note that technical editing may introduce minor changes to the text and/or graphics, which may alter content. The journal's standard [Terms & Conditions](#) and the [Ethical guidelines](#) still apply. In no event shall the Royal Society of Chemistry be held responsible for any errors or omissions in this *Accepted Manuscript* or any consequences arising from the use of any information it contains.

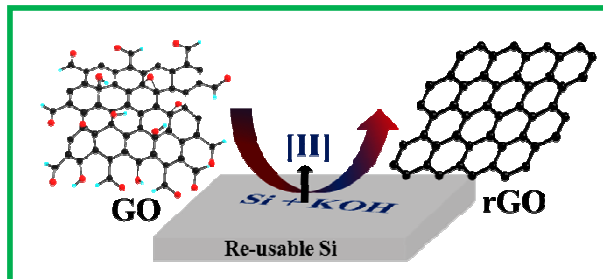


www.rsc.org/greenchem

Si-mediated fabrication of reduced graphene oxide and its hybrids for electrode materials

By Barun Kumar Barman and Karuna Kar Nanda*

We demonstrate Si-mediated environment friendly reduction of graphene oxide (GO) and the fabrication of hybrids electrode materials with the multiwall carbon nanotubes and nanofibers. The reduction of GO is facilitated by the nascent hydrogen generated by the reaction between Si and KOH. The overall process consumes 10 to 15 μm of Si each time and the same Si substrate can be used multiple times.



COMMUNICATION

Si-mediated fabrication of reduced graphene oxide and its hybrids for electrode materials

Cite this: DOI: 10.1039/x0xx00000x

Barun Kumar Barman and Karuna Kar Nanda*

Received 00th January 2012,

Accepted 00th January 2012

DOI: 10.1039/x0xx00000x

www.rsc.org/

Here, we demonstrate Si-mediated environment friendly reduction of graphene oxide (GO) and the fabrication of hybrids with the multiwall carbon nanotubes and nanofibers. The reduction of GO is facilitated by the nascent hydrogen generated by the reaction between Si and KOH at ~60 °C. The overall process takes 5 to 7 minutes and 10 to 15 μm of Si is consumed each time. We show that Si can be used multiple times and the rGO based hybrids can be used for the electrode materials.

Since the discovery, two-dimensional (2D) graphene sheet¹ has attracted world-wide attention among the experimentalist and theorist due to its excellent electrical, mechanical, thermal and optical properties.² Though it can be produced by micro-mechanical/liquid phase exfoliation of graphite,^{1,3} chemical vapour deposition⁴ and epitaxial growth,⁵ the chemical reduction of graphene oxide (GO)⁶ has great advantages because it can produce reduced GO (rGO) in large scale along with the fabrication of various kind of hybrid nanostructures. The chemical reduction of GO has been achieved by hydrazine,^{6(b) &(c)} dimethylhydrazine,^{6(d)} hydroquinone,^{6(e)} NaBH₄,^{6(f) &(g)} cysteine,⁷ p-phenylene diamine,⁸ glutathione,⁹ some environment-friendly reducing agent such as ascorbic acid, plant extraction, tannin, photochemical reduction,¹⁰ metal/acid or base¹¹ etc. rGO based hybrids with the carbon based nanostructures such as carbon nanotubes (CNTs) or carbon nanofibres (CNFs) have been synthesized *via* filtration,¹² layer-by-layer deposition (LbL),¹³ casting from inorganic solutions,¹⁴ electrophoretic deposition,¹⁵ Langmuir Blodgett techniques¹⁶ and chemical vapour deposition,¹⁷ etc. The rGO-CNT hybrids can be used for the advanced technology such as super-capacitors, conducting electrodes for solar-cells, fuel cell supporting materials, Li ion battery, sensing and catalytic application due to its large surface area, high thermal and electrical conductivity.¹⁸ Due to the high hydrophobic nature of the CNT/CNF, it is difficult to synthesize hybrids with the rGO (GO being hydrophilic nature) in

aqueous medium in bulk scale. Furthermore, large volume of minerals acid is required to remove excess metal impurities from rGO by metal mediated reduction of GO and the process is time consuming.

Herein, we demonstrate a rapid, an environment friendly and efficient way for the reduction of GO and rGO based hybrids with MWCNT/CNF at ~ 60 °C. Our strategy involves the use of commercially available Si in presence of KOH. The overall reduction process is complete within 5-7 minutes. For each experiment, 10 to 15 μm Si is consumed and therefore can be used for several reduction processes. The advantages associated with the reduction process are that it does not require any toxic chemical reagents or mineral acids to obtain high quality rGO and its hybrids.

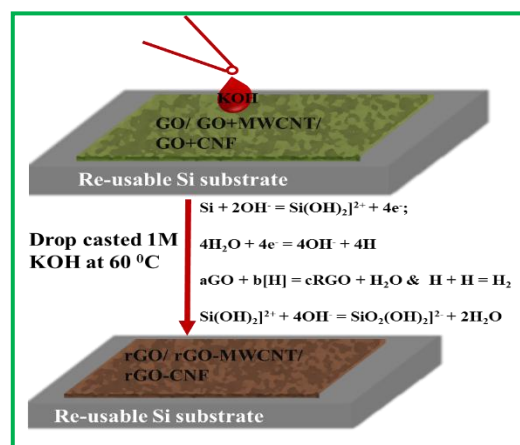


Fig.1 Schematic presentation of reduction of GO by reusable Si substrate.

Schematic of the fabrication process is shown in Fig. 1. First of all, GO are dispersed in dimethylformamide (DMF) solution and drop-casted onto the Si surface. Then KOH is added to it so that nascent

hydrogen is liberated and reduces the GO. In a typical experiment, 100 μl of GO solution was drop casted onto Si surface (1.0 cm^2) Si and dried under a lamp. Then 1M KOH ($\sim 1\text{ ml}$) solution was added to GO/Si at $60\text{ }^\circ\text{C}$. Black colour product was collected by simply washing with the de-ionized water and ethanol. To demonstrate the reuse of the Si substrate, we perform the reduction process 5 times using same Si substrate and named the samples as rGO-x ($x = 1, 2, 3, 4, 5$). For the synthesis of hybrids with MWCNTs and with CNFs, 1:4 ratio of GO and MWCNTs/CNFs is mixed thoroughly and placed on the top of the Si surface and follow the procedure as is the case of rGO (ESI-experimental section).

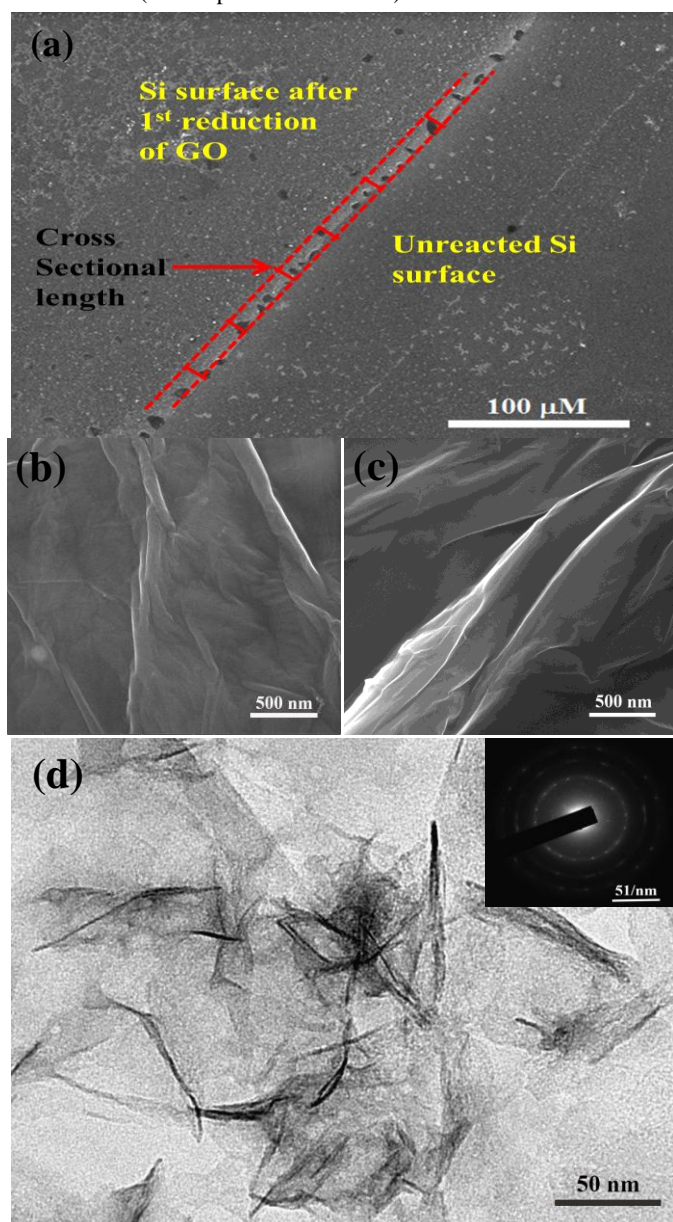


Fig.2 (a) Si surface after the 1st time used for GO reduction. (b & c) FESEM images of GO and rGO. (d) TEM image of. Inset image shows the SAED pattern of rGO, respectively.

As-synthesized rGO were characterized by scanning electron microscope (SEM), transmission electron microscope (TEM), X-ray

diffraction (XRD), X-ray photoelectron spectroscopy (XPS), energy dispersive X-ray spectroscopy (EDS), Raman and optical absorption studies. **Fig.2** (a) shows the SEM image of the edge portion of Si substrate after the first reduction of GO. Overall, the height between reacted and unreacted region is 10-15 μm which indicates that a few micrometer of Si is consumed each time. However, a single Si substrate can be used several times for reduction GO. The adsorb Si on rGO or hybrids is removed easily by successive washing with KOH solution followed by DI-water and ethanol. **Fig. 2** (b & c) show the SEM images of the curled, randomly aggregated solid sheets of GO and rGO. **Fig. 2** (d) and the inset show the TEM image and the selected area diffraction (SAED) pattern of rGO. The clear spots in SAED pattern due to the crystalline nature of rGO are clearly seen. In the case of GO, ring- like SAED pattern (ESI-1) is obtained due the polycrystalline & random orientation of graphene sheets and the presence of large amount of oxygen containing functional group at the edges and in the basal plane. After the removing the functional groups from graphene plane, crystalline nature is gained. A high resolution TEM (HRTEM) image of the edges of the rGO clearly shows 5-10 layers of graphene layer (ESI-2). The measured interlayer distance is approximately 0.36 nm similar with the van der Waals distance of the graphitic layer structures but smaller than the typical interlayer distance in GO (0.6–1.2 nm).¹⁹

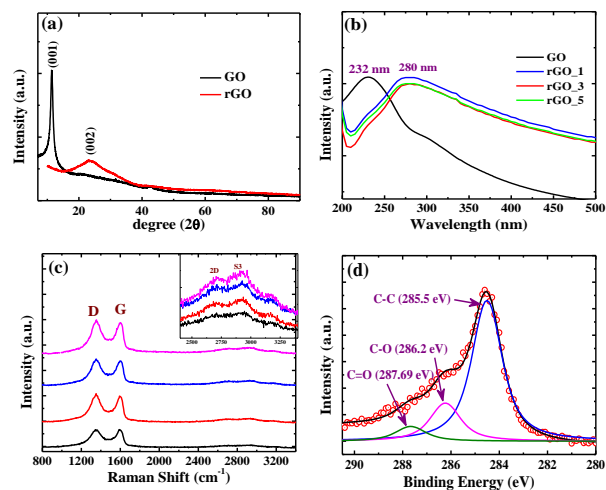


Fig.3 (a - c) XRD, UV- visible spectra and Raman spectra of GO and rGO and (d) XPS spectrum of rGO-1.

Fig. 3(a) shows the XRD patterns of GO and rGO. GO shows a sharp peak around $2\theta = 11.5^\circ$, which corresponds to a d-spacing of 0.76 nm for (001) plane indicating the presence of oxygen functionalities. The peak centered on at $2\theta = 24.5^\circ$ for rGO indicates the removal of a large number of oxygen-containing groups from GO resulting in the extensive conjugated sp^2 carbon network (i.e., the ordered crystal structure). The d-value is estimated to be 0.36 nm which is similar to the interlayer spacing obtained from HRTEM studies. The reduction of GO is also reflected in UV-visible and the Raman spectra as shown in Fig. 3(b) and 3(c), respectively. Generally, GO displays a strong absorption peak around 230 nm due to $\pi\text{-}\pi^*$ transition of aromatic C-C bonds and a weak peak around 300 nm due to $\text{n-}\pi^*$ transition of C=O bonds. The 230 nm peak is red

shifted to 280 nm which indicating the electronic conjugation within graphene sheet is recovered after the reduction of GO.⁶ Raman spectra as shown **Fig. 3** (c) reveal D and G peaks centred around 1349 and 1595 cm^{-1} for GO and 1351 and 1586 cm^{-1} for rGO, respectively. Apart from the shift of the G peak towards the graphitic peak (1581 cm^{-1}), the (I_D/I_G) intensity ratio increases slightly which is believed to be due to loss of oxygen containing functional group. There is an enhancement in the 2D and S3 peak intensity around at 2721.7 and 2927 cm^{-1} compared to the GO as shown in the inset of **Fig. 3**(c). This is in good agreement with the graphitic nature of rGO. We also investigate the UV-visible and Raman spectra of rGO-3 and rGO-5 (same Si substrate is used for 3rd and 5th reduction of GO) which clearly suggest that same Si can be used multiple times for the reduction of GO. To probe the amount of the reduction, both GO and rGO are characterized by XPS. The core level spectra of C1s of GO and rGO were deconvoluted into three major peaks with binding energy 284.5, 286.2 and 287.6 eV corresponding to the C-C/C=C (sp^2 bonding in the G), C-O (epoxy, alcohol, ester and acid groups) and C=O (carbonyl groups),¹¹ respectively. It is evident from **Fig. 3** (d) that the C-C bonds increase from 30% to 73.2%, while the C-O and C=O bonds decrease from 50.6% to 19.34% and 19.4% to 7%, respectively and the C/O ratio is 4.5:1.0 (**ESI-3**). Identical C/O ratio has also been realized from EDS study. The EDS spectrum of rGO shows the presence of C and O with 45.4 and 54.6% weight percentage for GO and 84.37 and 15.63% weight percentage for rGO. It may be noted that the C to O ratio varies from bottom to top of the films and the variation is ~6% (**ESI-6**).

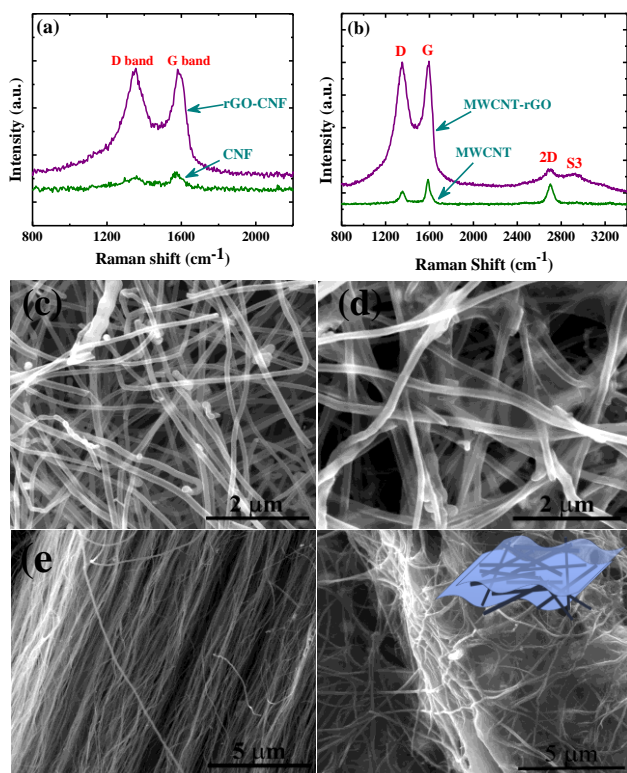


Fig. 4 (a & b) Raman spectra of rGO-CNF and rGO-MWCNT hybrids. (c & d) SEM images of CNF and rGO-CNF hybrids and (e & f) SEM images of MWCNT and MWCNT-rGO hybrids. Inset shows the schematic of the spatial sketch of MWCNT-rGO.

Fig. 4 (a & b) shows the Raman spectra of CNFs, MWCNTs, rGO-CNFs and rGO-MWCNTs hybrids. Both CNFs and MWCNTs show weak D and G bands around 1351 and 1580 cm^{-1} , but bands are strong for the hybrids as is the case for only rGO. The hybrids are also characterized by SEM. **Fig. 4** (c & d) shows the SEM images of bare CNFs and MWCNTs, while **Fig. 4** (e & f) displays the SEM images of the rGO-CNFs and rGO-MWCNTs hybrids. EDS analysis (**ESI-4**) indicates no any impurities except very low percentage of K (0.31% of K). Inset shows the schematic of the spatial sketch of MWCNT-rGO.

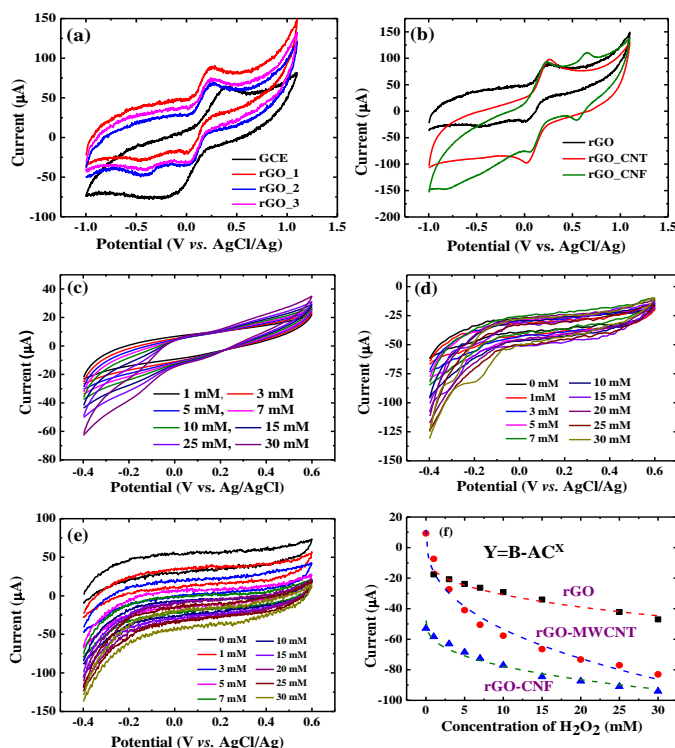


Fig. 5 (a) CV of rGO-1, rGO-3 and rGO-5 with 10 mM $\text{K}_4[\text{Fe}(\text{CN})_6]$ and 10 mM of KCl electrolyte. (b) CV of rGO, rGO/MWCNT and rGO/CNF. (c-e) CV recorded by successive addition of different concentration of H_2O_2 for rGO, rGO-CNF and rGO-MWCNT hybrids and (f) Current at -0.3 V vs concentration of H_2O_2 .

The conductivity of rGO and rGO-MWCNT hybrids is evaluated by four probe technique. The conductivity is found to be 96.25 S m^{-1} for rGO-MWCNT hybrids, which is 8 times higher compared to rGO (12.1 S m^{-1}). We also perform the electrochemical capacitance measurements for the rGO and rGO-MWCNT hybrids in 0.1 M Na_2SO_4 solution. The capacitance is 221 F g^{-1} for rGO-MWCNT hybrids, while it was 147 F g^{-1} for only rGO (**ESI-7**). Overall, the results suggest that rGO based hybrids have better electrical as well as electrochemical activity.

We further characterize the materials by electrochemical measurements to evaluate the electron transfer rate in the redox probe ferro/ferricyanide ($[\text{Fe}(\text{CN})_6]^{3-/4-}$) solution by cyclic voltammetry (CV).²⁰ The electron transfer mechanism in this redox couples is sensitive to the presence of oxygen containing functional

group, defects, surface microstructures and density of electronic states of the rGO. It is reported that the smaller peak-to-peak separation (ΔE_{p-p}) and higher the peak current in the redox system indicates the good kinetics on the electrode materials due good conductivity and fast electron transfer. Fig. 5 (a and b) show the CV of the rGO in the $\text{Fe}(\text{CN})_6^{3-/4-}$ redox probe system in presence of KCl electrolyte. Each of the electrode materials shows a well-defined cathodic and anodic redox peak current with a ΔE_{p-p} of 250 mV and higher current density as compared to the bare glassy carbon electrode (GCE) with a ΔE_{p-p} of 540 mV and a lower peak current density. The kinetics improves further when rGO based hybrids with the MWCNT and CNF are used. A ΔE_{p-p} of 190 and 230 mV with higher current density as compared to rGO are obtained for rGO-CNF and rGO-MWCNT hybrids, respectively. The lower values of ΔE_{p-p} observed in case of MWCNT and CNF modified rGO hybrids compared with the rGO. We also investigate the hydrogen peroxide (H_2O_2) sensing via electrochemical way. Fig. 5 (c-e) shows the CV response of different concentration of H_2O_2 for rGO, rGO-CNF and rGO-MWCNT hybrids at pH=7.2 of the electrolyte. When H_2O_2 is added gradually, the reduction peak increases in all the cases and at high concentration, it shows distinct reduction peak at -0.2 V. The current at -0.3 V vs concentration is shown in Fig. 5 (f). It is evident that rGO-MWCNT has the highest sensitivity in the lower concentration range and the current saturates at higher concentration of H_2O_2 . We fitted all the point by using nonlinear equation $Y=A-BC^x$, where A and B are the constants and C represents the concentration of the H_2O_2 . This indicates that the hybrids can be used as electrode materials for H_2O_2 sensing after suitable calibration.

In summary, we report a facile and one-step approach for GO reduction and fabrication of rGO based hybrids with MWCNTs and CNFs. Commercially available Si substrate is used for the reduction of GO in presence KOH solution. The overall process takes 5 to 7 minutes and 10 to 15 μm of Si is consumed each time. However, one Si substrate can be used multiple times for similar types of reaction. We also report the superiority of the hybrids over rGO as electrode materials for H_2O_2 sensing.

Acknowledgements

The authors acknowledge Department of Science and Technology (DST) for the financial support though DST-Nanomission.

Notes and references

^aMaterials Research Centre, Indian Institute of Science, Bangalore-560012, India. Fax: +91 80 2360 7316; Tel: +91 80 2293 2996; E-mail: nanda@mrc.iisc.ernet.in

Electronic Supplementary Information (ESI) available: [details of any supplementary information available should be included here]. See DOI: 10.1039/c000000x/

1 K. S. Novoselov, A. K. Geim, S.V.Morozov, D. Jiang, Y. Zhang, S.V. Dubonos, I. V. Grigorieva and A. A. Firsov, *Science*, 2004, **306**, 666–669.

2 (a) A. K. Geim and K. S. Novoselov, *Nat. Mater.*, 2007, **6**, 183–191; (b) K. S. Novoselov, A. K. Geim, S. V. Morozov, D. Jiang, M. I. Katsnelson, I. V. Grigorieva, S. V. Dubonos and A. A. Firsov, *Nature*, 2005, **438**, 197–200; (c) C. N. R. Rao, A. K. Sood, K. S. Subrahmanyam and A. Govindaraj, *Angew. Chem., Int. Ed.*, 2009, **48**, 7752–7777; (d) C. Lee, X. Wei, J. W. Kysar and J. Hone, *Science*, 2008, **321**, 385–388; (e) Y. Zhang, Y.-W. Tan, H. L. Stormer and P. Kim, *Nature*, 2005, **438**, 201–204; (f) A. A. Balandin, S. Ghosh, W. Bao, I. Calizo, D. Teweldebrhan, F. Miao and C. N. Lau, *Nano Lett.*, 2008, **8**, 902–907; (g) S. Latil and L. Henrard, *Phys. Rev. Lett.*, 2006, **97**, 036803; (h) A. K. Geim, *Science* **2009**, **324**, 1530–1534.

3. J. N. Coleman et al., *Nat. Nanotechnol.*, 2009, **3**, 563 – 568.

4.(a) K. S. Kim, Y. Zhao, H. Jang, S. Y. Lee, J. M. Kim, K. S. Kim, J. H. Ahn, P. Kim, J. Choi and B. H. Hong, *Nature*, 2009, **457**, 706–710; (b) P. W. Sutter, J. I. Flege and E. A. Sutter, *Nat. Mater.*, 2008, **7**, 406–411.

5. (a) C. Berger, Z. Song, T. Li, X. Li, A. Y. Ogbazghi, R. Feng, Z. Dai, A. N. Marchenkov, E. H. Conrad, P. N. First and W. A. de Heer, *J. Phys. Chem. B*, 2004, **108**, 19912–19916; (b) C. Berger, Z. Song, X. Li, X. Wu, N. Brown, C. Naud, D. Mayou, T. Li, J. Hass, A. N. Marchenkov and E. H. Conrad, et al., *Science*, 2006, **312**, 1191.

6. (a) S. Park, R. S. Ruoff, *Nat. Nanotechnol.*, 2009, **4**, 217–224; (b) S. Stankovich, D. A. Dikin, R. D. Piner, K. A. Kohlhaas, A. Kleinhammes, Y. Jia, Y. Wu, S. T. Nguyen and R. S. Ruoff, *Carbon* 2007, **45**, 1558–1565; (c) V. C. Tung, M. J. Allen, Y. Yang, R. B. Kaner, *Nat. Nanotechnol.* 2009, **4**, 25–29; (d) S. Stankovich, D. A. Dikin, G. H. B. Dommett, K. M. Kohlhaas, E. J. Zimney, E. A. Stach, R. D. Piner, S. T. Nguyen, R. S. Ruoff, *Nature*, 2006, **442**, 282–286; (e) G. X. Wang, J. Yang, J. Park, X. L. Gou, B. Wang, H. Liu and J. Yao, *J. Phys. Chem. C*, **2008**, **112**, 8192–8195; (f) H. J. Shin, K. K. Kim, A. Benayad, S. M. Yoon, H. K. Park, I. S. Jung, M. H. Jin, H. K. Jeong, J. M. Kim, J. Y. Choi and Y. H. Lee, *Adv. Func. Mater.*, 2009, **19**, 1987–1992; (g) Y. Si, E. T. Samulski, *Nano Lett.*, 2008, **8**, 1679–1682;

7. D. Zhang, X. Zhang, Y. Chen, C. Wang and Y. Ma, *Electrochim. Acta*, 2012, **69**, 364.

8. Y. Chen, X. Zhang, P. Yu and Y. Ma, *Chem. Commun.*, 2009, **30**, 4527–4529.

9. D. Zhang, X. Zhang, Y. Chen, C. Wang, Y. Ma, H. Dong, L. Jiang, Q. Meng and W. Hu, *Phys. Chem. Chem. Phys.*, 2012, **14**, 10899.

10. (a) Y. Lei, Z. Tang, R. Liaoa and B. Guo, *Green Chem.*, 2011, **13**, 1655–1658; (b) D. Mhamane, W. Ramadan, M. Fawzy, A. Rana, M. Dubey, C. Rode, B. Lefez, B. Hannyerd and S. Ogale, *Green Chem.*, 2011, **13**, 1990–1996; (c) X. H Li, J. S. Chen, X. Wang, M. E. Schuster, R. Schlögl and M. Antonietti, *ChemSusChem* 2012, **5**, 642–646; (d) J. Zhang, H. Yang, G. Shen, P. Cheng, J. Zhang and S. Guo, *Chem. Commun.*, 2010, **46**, 1112–1114.

11. (a) Z. Fan, K. Wang, T. Wei, J. Yan, L. Song and B. Shao, *Carbon*, 2010, **48**, 1686–1689; (b) Z. J. Fan, W. Kai, J. Yan, T. Wei, L. J. Zhi, J. Feng, Y. M. Ren, L. P. Song and F. Wei, *ACS Nano*, 2011, **5**, 191–198; (c) Y. Liu, Y. Li, M. Zhong, Y. Yang, Y. Wen and M. Wang, *J. Mater. Chem.*, 2011, **21**, 15449–15455; (d) R. Krishna, E. Titus, L. C. Costa, J. C. J. M. D. S. Menezes, M. R. P. Correia, S. Pinto, J. Ventura, J. P. Araujo, J. A. S. Cavaleiro, J. A. Gracio, *J. Mater. Chem.*, 2012, **22**, 10457–10459; (e) B. K. Barman, P. Mahanandia and K. K. Nanda, *RSC Advances*, 2013, **3**, 12621–12624; (f) B. K. Barman and K. K. Nanda, *Chem. Commun.*, 2013, **49**, 8949–8951.

12. Y. Xu, H. Bai, G. Lu, C. Li and G. Shi, *J. Am. Chem. Soc.* 2008, **130**, 5856–5857.

13.(a) H. R. Byon, S.W. Lee, S. Chen, P.T. Hammond, Y. Shao-Horn, *Carbon* 2011, **49**, 457–467; (b) D. Yu, L. Dai *J. Phys. Chem. Lett.* 2010, **1**, 467–470; (c) F. T. Lopez, A. M. Gomez, S. M. V. Diaz, M. L. G. Betancourt, N. P. Lopez, A. L. Elias, H. Muramatsu, R. C. Silva, S. Tsuruoka, Y. A. Kim, T. Hayashi, K. Kaneko, M. Endo and M. Terrones, *ACS Nano*, 2013, **7**, 10788–10798.

14. (a) X. Sun, X. Sun, J. Jin, X. Wang, D. Cai, M. J. Song, *Nanosci. Nanotechnol.* 2011, **11**, 5075–5082; (b) D. Cai, M. Song, C. Xu, C. Adv. *Mater.* 2008, **20**, 1706–1709.
15. S. B. Bon, L. Valentini, J. M. Kenny, L. Peponi, R. Verdejo, M. A. Lopez-Manchado, *Phys. Status Solidi A*, 2011, **207**, 2461–2466.
16. X. Li, G. Zhang, X. Bai, X. Sun, X. Wang, E. Wang & H. Dai, *Nat. Nanotechnol.* 2008, **3**, 538–542.
17. (a) Y. Wu, T. Zhang, F. Zhang, Y. Wang, Y. Ma, Y. Huang, Y. Liu, Y. Chen, *Nano Energy*, 2012, **1**, 820–827; (b) M. Q. Zhao, X. F. Liu, Q. Zhang, G. L. Tian, J. Q. Huang, W. Zhu and F. Wei, *ACS Nano*, 2012, **6**, 10759–10769; (c) T. Odedairo, J. Ma, Y. Gu, J. Chen, X. S. Zhao and Z. Zhu, *J. Mater. Chem. A*, 2014, **2**, 1418–1428.
18. (a) L. Qiu, X. Yang, X. Gou, W. Yang, Z. F. Ma, G. G. Wallace, D. Li, *Chem.; Eur. J.* 2010, **16**, 10653–10658; (b) T. K. Hong, D. W. Lee, H. J. Choi, H. S. Shin, B. S. Kim, *ACS Nano* 2010, **4**, 3861–3868; (c) V. C. Tung, L. M. Chen, M. J. Allen, J. K. Wassei, K. Nelson, R. B. Kaner, Y. Yang, *Nano Lett.* 2009, **9**, 1949–1955; (d) P. Han, Y. Yue, Z. Liu, W. Xu, L. Zhang, H. Xu, S. Donga, G. Cui, *Energy Environ. Sci.* 2011, **4**, 4710–4717; (e) H. Y. Jeong, D-S. Lee, H. K. Choi, D. H. Lee, J. E. Kim, J. Y. Lee, W. J. Lee, S. O. Kim and S. Y. Choi, *Appl. Phys. Lett.* 2010, **96**, 213105; (f) S. Nardecchia, D. Carriazo, M. L. Ferrer, M. C. Gutiérrez and F. del Monte, *Chem. Soc. Rev.*, 2013, **42**, 794–830; (g) D. D. Nguyen, N. H. Tai, S. Y. Chen and Y. L. Chueh, *Nanoscale*, 2012, **4**, 632–638.
19. K. A. Mkhoyan, A. W. Contryman, J. Silcox, D. A. Stewart, G. Eda, C. Mattevi, S. Miller and M. Chhowalla, *Nano Lett.*, 2008, **9**, 1058–1063.
20. (a) Z. Sofer, O. Jankovský, P. Šimek, L. Soferová, D. Sedmidubská and M. Pumera, *Nanoscale*, 2014, **6**, 2153–2160; (b) A. Y. Sheng Eng, Z. Sofer, P. Šimek, J. Kosina and M. Pumera, *Chem. Eur. J.* 2013, **19**, 15583–15592; (c) M. Pumera, *J. Mater. Chem. C*, 2014, **2**, 6454–6461.